2.N

Nuclear Physics A273 (1976) 243—252; © *North-Holland Publishing Co., Amsterdam*

^{6}Li ELASTIC SCATTERING ON ^{12}C, ^{16}O, ^{40}Ca, ^{58}Ni, ^{74}Ge, ^{124}Sn, ^{166}Er and ^{208}Pb AT $E(^{6}\mathrm{Li}) = 50.6$ MeV †

L. T. CHUA, F. D. BECCHETTI, J. JÄNECKE and F. L. MILDER

Physics Department, University of Michigan, Ann Arbor, Michigan, USA 48109

Received 28 June 1976

Abstract: The elastic scattering of ^{6}Li ions from a variety of targets, $A = 12$ to 208, has been measured at a bombarding energy of 50.6 MeV. The angular distributions are characteristic of strongly absorbed particles, such as ^{3}He and heavy ions, and less diffractive than for ^{4}He. A simple optical model with Woods-Saxon real and imaginary volume potentials is adequate to fit the data. Spin-orbit effects are not apparent in the data.

E NUCLEAR REACTIONS ^{12}C, ^{16}O, ^{40}Ca, ^{58}Ni, ^{74}Ge, ^{124}Sn, ^{166}Er, ^{208}Pb(^{6}Li, ^{6}Li), $E = 50.6$ MeV; measured $\sigma(\theta)$; deduced optical model parameters.

1. Introduction

Very few elastic scattering data have been published for ^{6}Li ions at bombarding energies greater than 30 MeV [refs. [1-7])]. The only extensive data above 30 MeV are on light mass targets such as ^{12}C, ^{16}O and ^{28}Si [refs. [3-7])]. The scarcity of data and hence optical model parameters at higher energies, particularly for heavier targets, severely limit the reliability of information obtained from the analysis of nuclear reactions involving ^{6}Li ions such as (d, ^{6}Li). The motivation for the present study was, in fact, to provide optical model parameters suitable for analysis of the latter reaction in heavy mass nuclei [8, 9]). Besides the pragmatic considerations, the study of ^{6}Li elastic scattering was deemed useful in its own right. Spin-orbit effects may be apparent since ^{6}Li has spin $S = 1$. Naively one would expect the ^{6}Li spin-orbit interaction to be reduced by $\frac{1}{3}$ compared to that of the deuteron owing to the increased projectile mass. Recent calculations dispute this and suggest that spin-orbit effects for heavy ions may be larger than expected [10-12]).

2. Experimental procedures

The experiments were performed with the University of Michigan 83 inch sector-focused cyclotron [13]). The beam was produced in an arc-type ion source by the sputtering action of a CO_2 plasma discharge on enriched lithium-6 fluoride †† melted

† Supported in part by USERDA, contract AEC AT(11-1)-2167.

†† Obtained from Isotope Sales Division, Union Carbide, Inc. Oak Ridge, Tenn. USA.

on a tantalum sleeve placed in the ion source [14]). This technique yielded 50 to 200 nA of extracted current, resulting in 10 to 50 nA energy-analyzed 50.6 MeV $^6Li^{++}$ beam on target, with $\Delta E(FWHM) \leq 20$ keV. The beam intensity was recorded with an electron-suppressed Faraday cup. It was also monitored with a solid-state detector set to observe elastic scattering at forward angles.

The scattered ^{6}Li ions were detected in either a movable solid-state detector or a dispersion-matched magnetic spectrometer equipped with a position-sensitive proportional counter in the focal plane. The latter detector consisted of a resistive-wire position counter, followed by two energy-loss counters, all in coincidence. This allowed a clean separation of ^{6}Li ions from other reaction products. The data were collected and displayed with an on-line PDP-15 computer.

The targets used were as follows: ^{12}C, natural carbon foils, 50 to 200 μg/cm^2; ^{16}O, natural calcium oxide or nickel oxide, 140 to 1145 μg/cm^2; ^{40}Ca, natural oxide, 1145 μg/cm^2; ^{58}Ni, natural metal foil, 220 and 450 μg/cm^2; ^{74}Ge, enriched oxide†, 100 μg/cm^2 on 40 μg/cm^2 carbon backing; ^{124}Sn, enriched metal †, 400 μg/cm^2 on 80 μg/cm^2 carbon backing; ^{166}Er, enriched oxide †, 158 μg/cm^2 on 40 μg/cm^2 carbon backing; ^{208}Pb, enriched metal [13]), 400 μg/cm^2 on 80 μg/cm^2 carbon backing. Although in most cases the target thicknesses were known from alpha-gauge or other measurements, the data were eventually normalized to forward angle Rutherford scattering cross sections.

The energy resolution, ΔE, in the solid state detector was typically 50 to 200 keV while for the spectrometer system ΔE was 20 to 100 keV. The latter was sufficient to separate adjacent isotope peaks and inelastic and elastic scattering at most angles. Most of the data for ^{12}C and ^{16}O were measured using the solid state detector while the majority of the other data were obtained with the magnetic spectrometer. The angular resolution, $\Delta\theta$, of the two systems (full width) was 0.2° to 2°, depending on the angle. The true beam axis was determined regularly from forward angle measurements on either side of the indicated 0° markers with a reduced spectrometer aperture of $\Delta\theta \approx 0.1°$.

Unless otherwise indicated, the relative accuracy of the data is ± 5 % or less, while the absolute error is ± 10 %, except the ^{12}C and ^{16}O data which are $\pm$ 30 % absolute.

3. Data

The experimental data are displayed in fig. 1 as a ratio with the Rutherford cross sections. The curves are optical model fits and will be discussed in sect. 4.

The ^{6}Li elastic scattering exhibits diffractive oscillations for the lighter mass targets ($A < 40$) which damp out with increasing target mass. The data appear to be characteristic of strongly absorbed projectiles [12]), such as ^{3}He and heavy ions (^{12}C, ^{16}O, etc.). We illustrate this more explicitly in fig. 2 where we compare the experimental elastic scattering of ^{3}He [ref. [15])], ^{4}He [ref. [16])], ^{6}Li (this work), ^{12}C [ref. [17])] and ^{16}O [ref. [18])] from ^{58}Ni at incident energies of about 10 MeV per nucleon. The distribution for the ^{6}Li projectile is intermediate to that for ^{3}He and ^{12}C or ^{16}O,

† Obtained from Isotope Sales Division, Union Carbide, Inc., Oak Ridge, Tenn. USA.

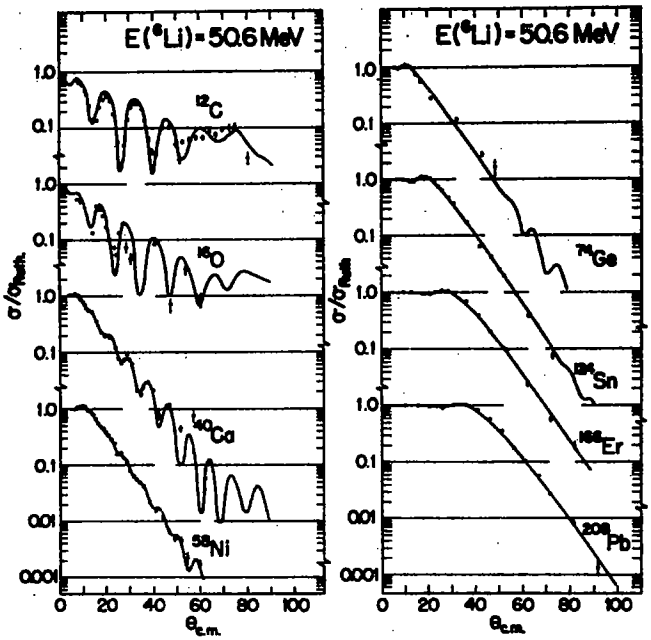

Fig. 1. Elastic scattering data for ^{6}Li at 50.6 MeV bombarding energy. The curves are optical model calculations using the parameters of table 1.

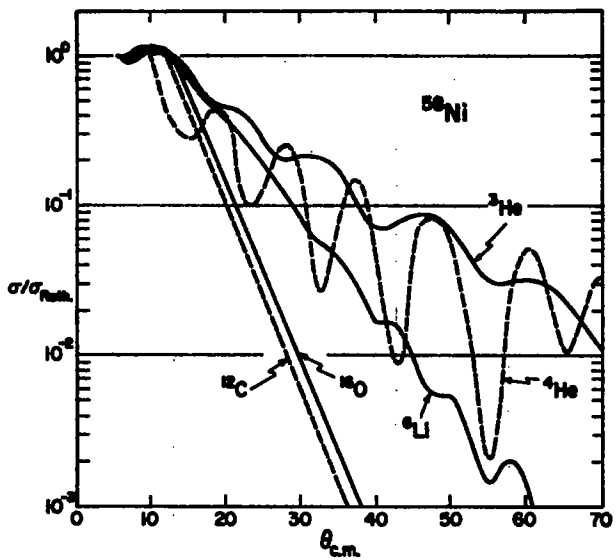

Fig. 2. Comparison of the elastic scattering from ^{58}Ni for the projectiles indicated. The bombarding energies are ^{3}He, 33 MeV [ref. [15])]; ^{4}He, 42 MeV [ref. [16])]; ^{6}Li, 50.6 MeV (this work); ^{12}C, 125 MeV [ref. [17])]; and ^{16}O, 158 MeV [ref. [18])]. The curves are fits to the data.

and quite unlike that for ^{4}He. The distribution for the tightly bound ^{4}He is very diffractive and uncharacteristic of the other composite ions. This feature is important if one wished to derive the ^{6}Li optical potential by "folding" in the known optical potentials of its constituents [19, 20]).

The characteristics of the ^{6}Li data, particularly for the heavier targets, suggests that some of the many semiclassical expressions derived for elastic scattering of strongly absorbed ions may be applicable. We have applied the simple semi-empirical relation derived in ref. [21]) for strong absorption

$$\sigma/\sigma_R = 1 - P_{abs}(D), \tag{1}$$

where

$$P_{abs}(D) = \begin{cases} 0, & \text{for } D \geqq D_0 \\ 1 - \exp\left((D-D_0)/\Delta\right), & \text{for } D < D_0. \end{cases} \tag{2}$$

The quantity D is the distance of closest approach for the classical Rutherford trajectory and is given by

$$D = \frac{zZe^2}{2E}\left(1 + \csc\tfrac{1}{2}\theta\right), \tag{3}$$

where z and Z are the charges of projectile and target, E is the c.m. energy and θ is the c.m. angle. It is also useful to define $d = D/(A_1^{\frac{1}{3}} + A_2^{\frac{1}{3}})$, where A_1 and A_2 are the projectile and target mass. The "quarter-point" radius, r_0, is the value of d corresponding to $\sigma/\sigma_R = \frac{1}{4}$.

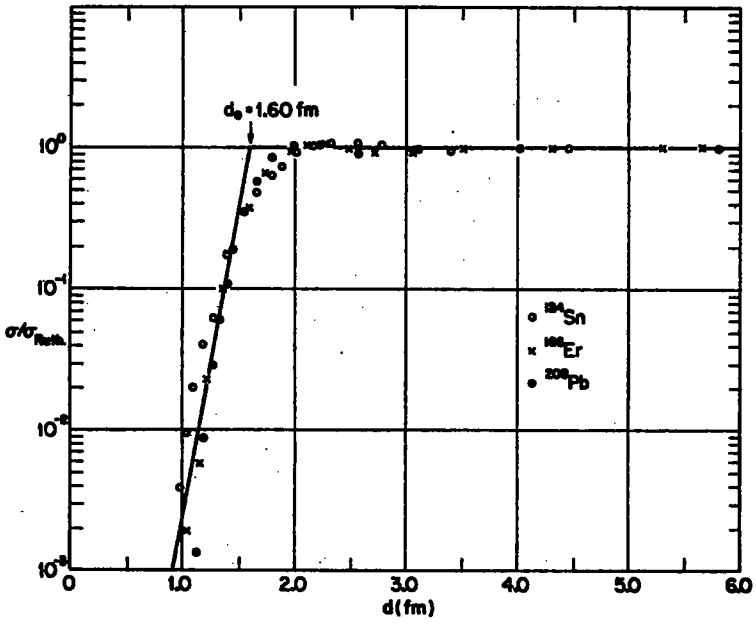

Fig. 3. A fit to the ^{6}Li elastic scattering data indicated using the semiclassical expression [eqs. (1)–(3)] with $d_0 = 1.60$ fm and $\Delta = 0.70$ fm.

We display in fig. 3 the data for ^{6}Li+^{124}Sn, ^{166}Er, and ^{208}Pb as a function of $d(\theta)$. The fit to the data shown yields $d_0 = 1.60$ fm and $\Delta \approx 0.7$ fm. This is to be compared with the values $d_0 = 1.68$ fm and $\Delta = 0.55$ fm obtained [21]) for ^{12}C and ^{16}O ions, $E \approx 60$ MeV and $A \approx 90$, and $d_0 = 1.50$ fm, $\Delta = 0.47$ fm obtained [22]) for ^{40}Ar+^{209}Bi, $E \approx 300$ MeV.

The increase in Δ for ^{6}Li compared to that for heavier ions indicates that the ^{6}Li absorption occurs more slowly with respect to the distance of closest approach. We then expect [21]) the diffuseness of the absorptive potential for ^{6}Li to be greater than that for heavier ions, which is indeed the case (sect. 4). These conclusions are altered somewhat by the presence of an attractive nuclear potential which distorts the classical orbits. Nonetheless, eqs. (1) to (3) provide a simple and useful description of the experimental data for heavier targets.

4. Optical model analysis

4.1. SIMPLE POTENTIALS

We have analyzed the ^{6}Li elastic data (fig. 2) using the conventional optical model with Woods-Saxon potentials [23]). The calculations were performed on an IBM 370/168 computer utilizing different computer codes [24, 25]). One of the codes [25]) permitted calculations with spin-orbit coupling for spin one particles. Corrections for the angular resolution were included.

Unfortunately, numerical accuracy was a problem even though all of the program codes were converted to run in double precision. This limited the extent of the calculations, particularly for heavier targets. Computing cost was also a factor. Parameter searches were therefore initially restricted to a simple volume Woods-Saxon potential (V_R, R_R, a_R, W_I, R_I, a_I) without spin-orbit coupling. The radii were taken to have the form $R_x = r_x A_2^{\frac{1}{3}}$ in accord with folding models [19, 20]).

Parameter sets based on those obtained by Chuev *et al.* [3]) ($E = 30$ MeV, $A = 12$ to 208) and Schumacher *et al.* [2]) ($E = 36$ MeV, $A = 12$ to 28) were used as starting parameters. The geometry parameters r_R, a_R, r_I and a_I were mapped in a coarse grid, and V_R and W_I adjusted to fit the data. As noted by other groups [6]) V_R and r_R are correlated with $V_R r_R^n \approx$ constant ($n \approx 1.7$). Also, V_R is determined only to the extent that the exterior part of the real potential is defined and the ^{6}Li phase shifts are correct at the nuclear surface. This results in an ambiguous determination of V_R. We therefore constrained V_R to be about six times the nucleon-nucleus potential [26]).

The parameters considered to be our "best fit" parameters given the above constraints are listed in table 1. These parameters give a good description of the experimental data. In addition they were found to result in good fits to (d, ^{6}Li) data when used [8, 9]) in distorted-wave codes. Although our optical model analysis was by no means exhaustive, the ^{6}Li parameters in table 1 should be adequate for most applications.

We also considered potentials of the form used by Poling *et al.* [6]) for ^{6}Li+^{12}C.

TABLE 1

"Best fit" optical model parameters, $E(^6\text{Li}) = 50.6$ MeV

Target	V_R [a] (MeV)	r_R (fm)	a_R (fm)	W_I (MeV)	r_I (fm)	a_I (fm)	σ_R [b] (fm²)	$r_{s.a.}$ [c] (fm)	r_0 [d] (fm)	J_R/A [e] (MeV/fm³)	J_I/A [e] (MeV/fm³)
^{12}C	214	1.30	0.70	26.8	1.70	0.90	138	1.61		505	140
^{16}O	210	1.30	0.70	25.0	1.70	0.90	148	1.59		469	123
^{40}Ca	244	1.30	0.70	23.5	1.70	0.90	192	1.49	1.32	464	99
^{58}Ni	232	1.30	0.70	20.0	1.70	0.90	206	1.42	1.49	423	81
^{74}Ge	240	1.30	0.65	18.0	1.70	0.90	216	1.38	1.40	420	72
^{124}Sn	240	1.30	0.65	16.0	1.70	0.90	234	1.27	1.51	404	61
^{166}Er	240	1.30	0.65	14.0	1.70	0.90	229	1.17	1.51	397	52
^{208}Pb	240	1.30	0.65	12.0	1.70	0.90	219	1.08	1.52	394	44

[a]) The optical potentials $V(r)+V_C(r)+iW(r)$ are defined as $V(r) = -V_R f(r, R_R, a_R)$ and $W(r) = -W_I f(r, R_I a_I)$, where $f(r, R_x, a_x) = [1+\exp(r-R_x)/a_x]^{-1}$ and $R_x = r_x A_2^{\frac{1}{3}}$ where A_2 is the target mass number. The potential $V_C(r)$ is taken to be the Coulomb potential due to a uniformly charged sphere with radius $R_C = 1.40\, A_2^{\frac{1}{3}}$ fm [see ref. [26])].

[b]) The calculated total reaction cross section in fm² (1 fm² = 10 mb) using the potentials listed.

[c]) The strong absorption radius $r_{s.a.}$ is defined by $\sigma_R = \pi R^2$ where $R = r_{s.a.}(A_1^{\frac{1}{3}}+A_2^{\frac{1}{3}})$.

[d]) The classical radius r_0 (eq. (3)) corresponding to the quarter-point angle in the σ/σ_R distribution where $D(\sigma/\sigma_R = \frac{1}{4}) = r_0(A_1^{\frac{1}{3}}+A_2^{\frac{1}{3}})$.

[e]) Volume integral per target nucleon [see ref. [19])].

These have surface absorption. Although fits comparable to the "best fit" set of table 1 could be obtained, no obvious preference for this type of potential was indicated.

4.2. SPIN-ORBIT EFFECTS

Calculations were also performed using a standard Thomas derivative-type $\boldsymbol{l}\cdot\boldsymbol{s}$ spin-orbit potential [23]). The influence of such a potential is shown in fig. 4. The main effect is to increase the magnitude of the oscillations at large angles. As this can usually be compensated by slight adjustments in the other parameters, particularly those of the absorptive potential, we conclude that the presence of a moderate spin-orbit potential cannot be unambiguously determined from the present data. We can, however, set an upper limit of about 10 MeV for $V_{s.o.}$ ($r_{s.o.} = 1.2$ fm, $a_{s.o.} = 1.7$ fm; see fig. 4). We conclude that spin-orbit effects for ^{6}Li projectiles are not large, at least in the elastic channels.

Recently polarized ^{6}Li beams have become available [27]) and some direct measurements of elastic asymmetries have been performed [27, 28]). While large asymmetries ($\langle iT_{11}\rangle \approx 0.5$) are observed at 20 MeV bombarding energy for light targets such as ^{12}C and ^{16}O, at most only slight effects are observed for targets heavier than ^{28}Si. In particular, $\langle iT_{11}\rangle$ is less than 0.1 for ^{58}Ni. These results are not inconsistent with our analysis as the spin-orbit potentials required [28]) to give these asymmetries have only a slight effect on the elastic scattering of unpolarized ^{6}Li projectiles. The situation is very similar to that observed for ^{3}He and tritons [29, 30]), which like ^{6}Li are strongly absorbed projectiles. It is in contrast to that for protons and deuterons where spin-orbit potentials are already needed to fit the elastic scattering [26, 31]). In

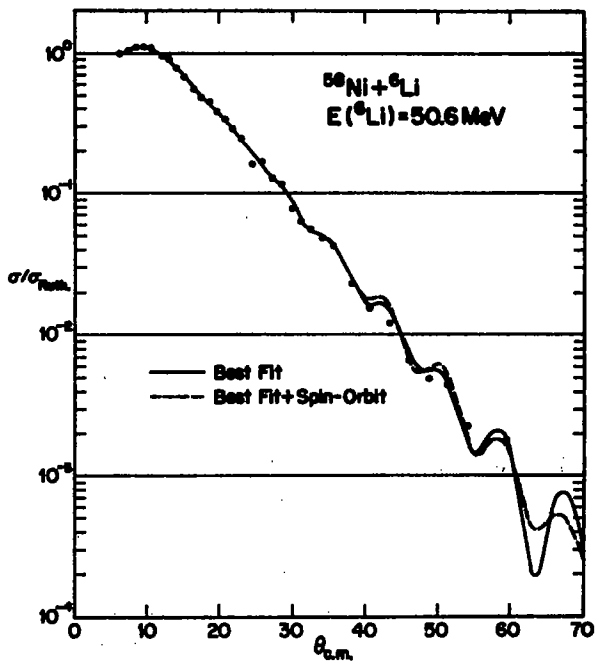

Fig. 4. Comparison of calculations with and without an $l \cdot s$ spin-orbit potential for ^{6}Li+^{58}Ni. The potential of table 1 was used with $V_{s.o.} = 6$ MeV, $r_{s.o.} = 1.20$ fm, $a_{s.o.} = 0.70$ fm, and $V_{s.o.} = 0$ MeV, respectively. The spin-orbit form factor is of the conventional Thomas type [23]).

the former instances one must then rely on direct polarization measurements to determine the presence of a spin-orbit interaction [29, 30]).

The lack of strong spin-orbit effects in ^{6}Li elastic scattering suggest that in first order they may also be neglected in DWBA analyses of most transfer reactions.

4.3. MASS DEPENDENCE

The dependence of the parameter W on target mass number $A(=A_2)$ for the "best fit" potentials is presented in fig. 5. We find that $W_I \approx 26-0.075A$ MeV. Note that the corresponding geometry parameters r_I and a_I have been set at fixed values. The volume integrals J_I/A of the absorptive potential (table 1) exhibit a decrease with increasing A similar to W_I, indicating that the relative absorption per nucleon decreases with target mass. One may ascribe this result to the fact that the surface regions are dominant in the absorptive processes. This is confirmed by the near equivalency of volume and surface form factors for the imaginary potentials (subsect. 4.1).

The real-well depths, V_R, and the corresponding volume integrals J_R/A do not show a marked mass dependence (table 1) although this is due in part to the presence of the Coulomb potential. There is no evidence for a symmetry potential [23, 26]),

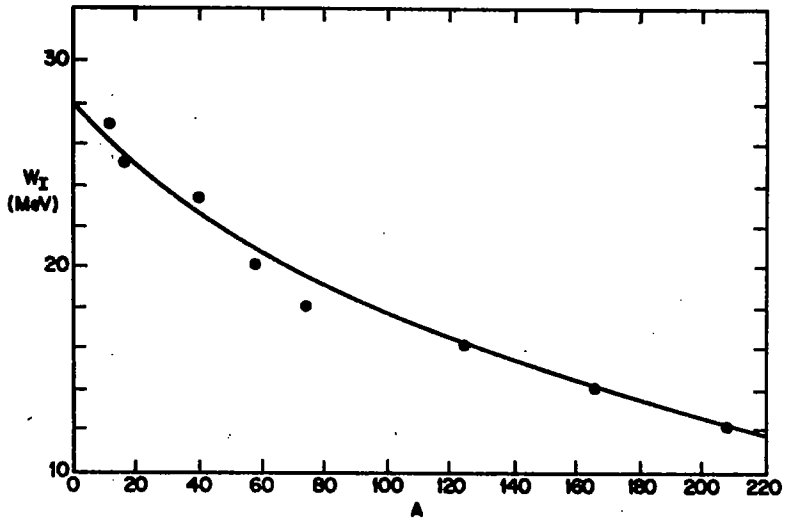

Fig. 5. Mass dependence of the strength of the absorptive potential, W_I, for the parameter set of table 1.

proportional to $(N-Z)/A$. Such a potential is not expected since ^{6}Li has an isospin of zero. The fact that the volume integrals per nucleon J_R/A (table 1) are comparable to those obtained for nucleon-nucleus scattering [26]) is a result of our constraints on V_R (subsect. 4.1).

4.4. ENERGY DEPENDENCE

A comparison of the ^{6}Li potentials determined at 50.6 MeV energy with those from analyses at lower energies enables one to determine the energy dependence of the potential parameters. This is meaningful only for common geometry parameters and family sets, though, owing to ambiguities. We have therefore used our "best fit" set as a basis for determining potential parameters at other bombarding energies. Specifically, we have reanalyzed the ^{58}Ni and ^{124}Sn data of Chuev *et al.* [3]) at 30 MeV bombarding energy by readjusting V_R and W_I. The results indicate at most a slight decrease in V_R with increasing ^{6}Li energy ($dV_R/dE \leqq 4$). This is comparable to that observed for nucleon-nucleus scattering [26]) where $dV_R/dE_p \approx 0.32$ which implies $dV_R/dE \approx 2$ for mass-6 projectiles. The results for the imaginary potential were inconclusive. It appears, however, that the parameters of table 1 can be extrapolated well above and below 50 MeV ^{6}Li bombarding energy.

4.5. TOTAL REACTION CROSS SECTIONS

Total reaction cross sections, σ_R, have been calculated and are indicated in table 1. We have also calculated the phenomenological strong absorption radius, $r_{s.a.}$, defined by

$$\sigma_R = \pi R^2, \tag{4}$$

with $R \equiv r_{s.s.}(A_1^{\frac{1}{3}}+A_2^{\frac{1}{3}})$. The quantity $r_{s.s.}$ is observed to scale with the strength of the absorptive potential W_I, e.g. $r_{s.s.} \approx 1.61$ fm for $A = 12$ while $r_{s.s.} \approx 1.08$ fm for $A = 208$ (table 1). Our values for $r_{s.s.}$ are comparable to those determined [12]) for heavier ions such as ^{12}C and ^{16}O. The calculated reaction cross sections, σ_R, for ^{6}Li and other heavy ions are about twice as large as those for nucleon-nucleus scattering [26]) at comparable energies per nucleon.

5. Conclusions

We conclude from our analysis of 50.6 MeV ^{6}Li elastic scattering from a range of nuclei that ^{6}Li scattering has characteristics similar to those of ^{3}He and heavier ions such as ^{12}C and ^{16}O. Spin-orbit effects are not apparent in the elastic scattering data. The absorptive part of the optical potential exhibits a noticeable decrease with increasing target mass but little energy dependence. The real potential depth shows little dependence on target mass and a slight decrease with increasing bombarding energy, if any.

The authors thank the staff of the cyclotron laboratory for their help. We also thank P. Schwandt, R. DeVries and G. R. Satchler for their assistance in obtaining copies of the computer codes used in the analysis.

References

1) K. Bethge, C. M. Fou and R. W. Zurmühle, Nucl. Phys. A123 (1969) 521
2) P. Schumacher, N. Veta, H. H. Duhm, K. I. Kubo and W. J. Klages, Nucl. Phys. A212 (1973) 573
3) V. I. Chuev *et al.*, J. de Phys. 32 Suppl. 11–12 (1971) C6–157; C6-161
4) G. Bassani, N. Saunier, B. M. Traore, J. Raynal, A. Foti and G. Pappalardo, Nucl. Phys. A189 (1972) 353
5) P. K. Bindal, K. Nagatani, M. J. Schneider and P. D. Bond, Phys. Rev. C9 (1974) 2154
6) J. E. Poling, E. Norbeck and R. R. Carlson, Phys. Rev. C13 (1976) 648
7) J. G. Cramer, R. M. DeVries, D. A. Goldberg, M. S. Zisman and C. F. Maguire, submitted for publication
8) F. D. Becchetti and J. Jänecke, Phys. Rev. Lett. 35 (1975) 268
9) F. L. Milder, J. Jänecke and F. D. Becchetti, Clustering phenomena in nuclei II, ed. D. A. Goldberg *et al.* (USERDA report ORD-4856-26, 1975) p. 409 and Nucl. Phys., to be published; F. L. Milder, thesis (University of Michigan, 1975)
10) W. J. Thompson, in Reactions between complex nuclei, vol. 1, ed. R. L. Robinson *et al.* (North-Holland, Amsterdam, 1974) p. 14
11) C. Chasman, private communication
12) R. H. Venter and W. E. Frahn, Ann. of Phys. 27 (1964) 401
13) W. C. Parkinson *et al.*, Nucl. Instr. 119 (1974) 61
14) E. D. Hudson and M. L. Mallory, private communication; D. J. Clark, private communication
15) M. E. Cage *et al.*, Nucl. Phys. A183 (1972) 449; P. P. Urone, L. W. Put and B. W. Ridley, Nucl. Phys. A186 (1972) 344
16) N. Baron, R. F. Leonard and W. M. Stewart, Phys. Rev. C4 (1971) 1159
17) J. Alster and H. E. Conzett, Phys. Rev. 136 (1964) B1023
18) J. A. McIntyre, S. D. Baker and T. L. Watts, Phys. Rev. 116 (1959) 1212

19) G. W. Greenlees, G. J. Pyle and Y. C. Tang, Phys. Rev. 171 (1968) 1115;
P. Mailandt *et al.*, Phys. Rev. C8 (1973) 2189
20) S. G. Kadmenskii, Sov. J. Nucl. Phys. 8 (1969) 284;
J. W. Watson, Nucl. Phys. A198 (1972) 129
21) P. R. Christensen, V. I. Manko, F. D. Becchetti, Jr. and R. J. Nickles, Nucl. Phys. A207 (1973) 33
22) J. R. Birkelund *et al.*, Phys. Rev. C13 (1976) 133;
H. C. Britt *et al.*, Phys. Rev. C13 (1976) 1483
23) P. E. Hodgson, Optical model of elastic scattering (Oxford University Press, 1963)
24) F. G. Perey, Program JIB3 (unpublished)
25) P. Schwandt, Program SNOOPY5 (unpublished)
26) F. D. Becchetti, Jr. and G. W. Greenlees, Phys. Rev. 182 (1969) 1190
27) E. Steffens *et al.*, Nucl. Instr. 124 (1975) 601
28) W. Weiss *et al.*, Phys. Lett. 61B (1976) 237
29) J. B. A. England *et al.*, Nucl. Phys. A165 (1971) 277
30) R. A. Hardekopf, L. R. Veeser and P. W. Keaton, Jr., Phys. Rev. Lett. 35 (1975) 1623
31) L. D. Knutson and W. Haeberli, Phys. Rev. Lett. 30 (1973) 986